HHS Public Access

Author manuscript

Nat Metab. Author manuscript; available in PMC 2020 January 08.

Published in final edited form as:

Nat Metab. 2019 July ; 1(7): 676–687. doi:10.1038/s42255-019-0082-3.

Glutamine independence is a selectable feature of pluripotent stem cells

Santosha A. Vardhana[1,2], **Paige K. Arnold**[2,3,4], **Bess P. Rosen**[5], **Yanyang Chen**[2,3], **Bryce W. Carey**[6], **Danwei Huangfu**[5], **Carlos Carmona-Fontaine**[7], **Craig B. Thompson**[1,2], **Lydia W.S. Finley**[2,3,*]

[1]Cancer Biology and Genetics Program, Memorial Sloan Kettering Cancer Center, New York, New York, USA

[2]Center for Epigenetics Research, Memorial Sloan Kettering Cancer Center, New York, New York, USA

[3]Cell Biology Program, Memorial Sloan Kettering Cancer Center, New York, New York, USA

[4]Louis V. Gerstner, Jr., Graduate School of Biomedical Sciences, Memorial Sloan Kettering Cancer Center, New York, New York, USA

[5]Developmental Biology Program, Memorial Sloan Kettering Cancer Center, New York, New York, USA

[6]Laboratory of Chromatin Biology and Epigenetics, The Rockefeller University, New York, New York, USA

[7]Center for Genomics & Systems Biology, Department of Biology, New York University, New York, New York, USA

Abstract

Most rapidly proliferating mammalian cells rely on the oxidation of exogenous glutamine to support cell proliferation. We previously found that culture of mouse embryonic stem cells (ESCs) in the presence of inhibitors against MEK and GSK3β to maintain pluripotency reduces cellular reliance on glutamine for tricarboxylic acid (TCA) cycle anaplerosis, enabling ESCs to proliferate in the absence of exogenous glutamine. Here we show that reduced dependence on exogenous glutamine is a generalizable feature of pluripotent stem cells. Enhancing self-renewal, through either overexpression of pluripotency-associated transcription factors or altered signal transduction, decreases the utilization of glutamine-derived carbons in the TCA cycle. As a result,

*Correspondence should be addressed to L.W.S.F. (finleyl@mskcc.org).

Author Contributions

S.A.V. and L.W.S.F. conceived the study. S.A.V., P.K.A and L.W.S.F. performed all experiments with assistance from Y.C. B.C. assisted with reprogramming experiments. B.P.R. and D.H. performed human ESC experiments. C.C-F. performed immunofluorescence and image analysis. C.B.T. provided additional work in conception and study guidance. S.A.V. and L.W.S.F. wrote the manuscript.

Competing Interests Statement

C.B.T. is a founder of Agios Pharmaceuticals and a member of its scientific advisory board. He also previously served on the board of directors of Merck and Charles River Laboratories.

cells with the highest potential for self-renewal can be enriched by transient culture in glutamine-deficient media. During pluripotent cell culture or reprogramming to pluripotency, transient glutamine withdrawal selectively leads to the elimination of non-pluripotent cells. These data reveal that reduced dependence on glutamine anaplerosis is an inherent feature of self-renewing pluripotent stem cells and reveal a simple, non-invasive mechanism to select for mouse and human pluripotent stem cells within a heterogeneous population during both ESC passage and induced pluripotent cell reprogramming.

Introduction

When induced to proliferate in culture, mammalian cells rewire metabolic pathways to support the anabolic demands of cell growth. Cells take up high levels of glucose and glutamine, which are used to generate the metabolic building blocks, reducing equivalents and energy required to duplicate biomass prior to cell division[1]. Consequently, exogenous supplies of both glucose and glutamine are essential to sustain rapid proliferation of most cultured cell lines[1]. While proliferating cells of all lineages share many common metabolic features, most notably elevated glycolysis and glutaminolysis, recent evidence demonstrates that there is not one single mode of proliferative metabolism. Rather, cells can engage multiple routes of nutrient acquisition and catabolism to support survival and proliferation[2]. Several factors contribute to this metabolic diversity, including cell lineage, genetic makeup and environmental conditions[3]. This raises the intriguing possibility that metabolic manipulation can provide selective pressures that promote or antagonize the proliferation of distinct cell types in a predictable manner.

Metabolites serve many roles beyond anabolic building blocks. Metabolites also serve as signals or effectors that affect myriad cellular processes, including signal transduction, stress response pathways and chemical modification of proteins and nucleic acids[4,5]. Consequently, regulation of cellular metabolism has emerged as a mechanism to influence cell fate decisions beyond proliferation. In particular, many of the enzymes that modify DNA and histones require metabolites as necessary co-substrates, raising the possibility that metabolic fluctuations shape the chromatin landscape and, in turn, affect gene expression programs[4,6]. Indeed, pathological accumulation of certain metabolites in many malignancies is sufficient to block differentiation and promote transformation by disrupting the normal dynamic chromatin regulation of progenitor cells[7].

Collectively, these findings suggest that how a cell solves the problem of proliferative metabolism may have consequences for the regulation of cell identity. The link between proliferation and cell identity is especially critical in pluripotent stem cells, which proliferate rapidly in culture while retaining the capacity to differentiate into all three lineages of the developing embryo. Pluripotent stem cells utilize glucose and glutamine to fuel proliferation, and perturbations in the metabolism of these nutrients can alter both survival and differentiation[8-11]. Notably, glucose-derived acetyl-CoA, the substrate for histone acetyltransferases, and glutamine derived α-ketoglutarate (αKG), a co-substrate of αKG-dependent dioxygenases including the Tet family of methylcytosine oxidases and the Jumonji-domain containing family of histone demethylases, contribute to the regulation of

the chromatin landscape, thereby influencing the balance of self-renewal vs differentiation[8,12-14].

Given the emerging links between proliferative metabolism and cell identity, we speculated that we could exploit the specific metabolic requirements of particular cell types to favor the enrichment of cells with the highest capacity for self-renewal. Mouse embryonic stem cells (ESCs) cultured under conventional conditions including serum and leukemia inhibitory factor (LIF; hereafter S/L) exhibit heterogeneous expression of key pluripotency transcription factors that denote cells with variable propensity for differentiation[15,16]. Addition of inhibitors against MEK and GSK3β ('2i') drives cells into a naïve "ground state" of pluripotency in which cells express relatively homogenous levels of pluripotency transcription factors and are resistant to spontaneous differentiation[17]. We previously showed that addition of 2i to mouse ESCs rewired intracellular metabolic pathways without altering proliferation rate[8]. In particular, 2i-cultured ESCs decreased glutamine oxidation and increased glucose oxidation, enabling an increase in the ratio of αKG/succinate that has been mechanistically linked to the regulation of chromatin and cell identity in a variety of contexts[8,18-20]. However, whether altered metabolic profiles are a specific consequence of altered signal transduction or a general feature of self-renewing ESCs remains an open question. Here we address this issue and reveal that reduced reliance on exogenous glutamine is a fundamental feature of highly self-renewing ESCs. Accordingly, both mouse and human pluripotent stem cells are able to survive and be enriched by transient culture in glutamine-deficient medium. These results demonstrate that defined metabolic profiles are an inherent feature of pluripotent stem cell identity and provide a rationale for the use of metabolic interventions as a method to manipulate heterogeneity in stem cell populations.

Results

Glutamine anaplerosis is reduced in highly self-renewing ESCs

In proliferating mammalian cells *in vitro*, glutamine is the major source of carbon for tricarboxylic acid (TCA) cycle intermediates[1]. Consequently, most cell lines including ESCs depend on exogenous glutamine for growth and proliferation[1,8,10]. One notable exception is 2i-cultured mouse ESCs in the ground state of pluripotency, which can sustain proliferation in the absence of exogenous glutamine[8]. Previously, we found that addition of 2i reduces the contribution of glutamine-derived carbons to TCA cycle intermediates while increasing the contribution of glucose-derived carbons, thereby reducing reliance on exogenous glutamine to support TCA cycle anaplerosis[8]. To determine whether the effects of 2i on mouse ESC metabolism are a specific consequence of MEK/GSK3β inhibition or a general feature of the metabolic requirements of self-renewing pluripotent cells, we utilized alternative methods to drive ESCs into the ground state of pluripotency. First, we took advantage of a chimeric LIF receptor engineered to respond to granulocyte colony-stimulating factor (GCSF) and harboring a mutation at tyrosine 118 to impair negative feedback by Socs3[21]. Upon treatment with GCSF, cells expressing this chimeric receptor exhibit elevated and sustained JAK/STAT3 signaling (Supplementary Fig. 1a) and are stabilized in the naïve state of pluripotency regardless of the presence of differentiation-inducing stimuli[22].

To assess glucose and glutamine utilization in these cells, we used gas chromatography-mass spectrometry to trace the fate of uniformly ^{13}C-labeled glucose or glutamine. In addition to enhancing expression of the Stat3 target gene *Tfcp2l1* and key transcription factors associated with naïve pluripotency[23] (Supplementary Fig. 1b), GCSF treatment induced metabolic alterations similar to those triggered by 2i. Specifically, GCSF increased the fraction of TCA cycle metabolites derived from oxidative decarboxylation of glucose-derived pyruvate (m+2 labeled isotopologues) and decreased the fraction of metabolites derived from glutamine catabolism (Fig. 1a-d, Supplementary Table 1). Whereas more than 80% of glutamate is derived from glutamine in control ESCs, in line with other cultured mammalian cells, GCSF reduced the fraction of glutamate derived from glutamine to 60% suggesting that GCSF-cultured ESCs can generate glutamate from sources other than glutamine (Fig. 1d, Supplementary Table 1). Indeed, when deprived of exogenous glutamine, GCSF-cultured ESCs were able to use glucose and other anaplerotic substrates to maintain intracellular pools of glutamate (Supplementary Fig. 1c, Supplementary Table 1).

Both MEK/GSK3β inhibition and JAK/STAT3 activation promote naïve pluripotency by altering signal transduction. To determine whether direct activation of pluripotency gene networks is sufficient to rewire intracellular metabolic pathways, we ectopically expressed pluripotency-associated transcription factors Klf4 and Nanog (Supplementary Fig. 1d). Expression of either transcription factor is sufficient to enhance self-renewal[24-26] and induce expression of target genes associated with naïve pluripotency[27,28] (Supplementary Fig. 1e). Similar to MEK/GSK3β inhibition and JAK/STAT3 activation, overexpression of Klf4 or Nanog increased the fraction of TCA cycle intermediates generated from glucose-derived carbons (Fig. 1e, Supplementary Table 1) while decreasing the fraction of TCA cycle intermediates derived from glutamine (Fig. 1f, Supplementary Table 1). Under conditions of reduced glutamine anaplerosis, pyruvate carboxylase can partially compensate to maintain TCA cycle anaplerosis[29]. Accordingly, both JAK/STAT3-stimulated and Nanog/Klf4-expressing cells exhibited an increase in glucose-derived anaplerosis through pyruvate carboxylase (m+3 isotopologues), further underscoring the reduced reliance on glutamine anaplerosis in cells with enhanced pluripotency networks (Supplementary Fig. 1f-h, Supplementary Table 1).

Together, these results suggest that interventions that enhance ESC self-renewal alter the balance of glucose and glutamine utilization in cells independently of changes in culture conditions or proliferation rates (Supplementary Fig. 1i,j). We have previously represented this metabolic shift—marked by reduced glutamine anaplerosis coupled with enhanced contribution of glucose-derived carbons to TCA cycle metabolites—as a change in the ratio of α-ketoglutarate to succinate[8]. Both JAK/STAT3 induction and Nanog overexpression increase cellular αKG/succinate ratios, while Klf4, which has a more modest effect on glucose and glutamine utilization under routine culture conditions, had no notable effect on this ratio (Fig. 1g,h, Supplementary Table 1).

We next asked whether the αKG/succinate ratio varies in correlation with the inherent self-renewal potential of ESCs. The significant population heterogeneity of ESCs cultured under conventional serum/LIF (S/L) conditions provided an opportunity to determine whether the functional heterogeneity of ESCs is accompanied by metabolic heterogeneity. To this end,

we utilized ESCs harboring a GFP reporter at the endogenous *Nanog* locus[30] to sort out cells with the lowest and highest expression of Nanog (Fig. 1i, left). These Nanog-GFP cells have previously been used to illustrate that "Nanog Low" cells are more prone to differentiate than their "Nanog High" counterparts[30,31]. Because of the inherent metastability of S/L-cultured ESCs, within three days of sorting both "Nanog Low" and "Nanog High" sorted populations had begun to re-establish the variable Nanog expression that characterizes S/L-cultured ESCs (Fig. 1i, right). Nevertheless, the ratio of αKG/succinate was significantly different in the two populations, with Nanog High cells characterized by an elevated αKG/succinate ratio consistent with their enhanced capacity for self-renewal (Fig. 1j, Supplementary Table 1). Further supporting a tight correlation between the αKG/succinate ratio and ESC self-renewal, the αKG/succinate ratio increased progressively from Nanog-low to Nanog-intermediate and Nanog-high populations (Supplementary Fig. 1k, Supplementary Table 1).

ESCs with enhanced self-renewal exhibit reduced dependence on exogenous glutamine

We next probed the functional outcome of reduced glutamine anaplerosis in order to further test whether altered proliferative metabolism is an inherent feature of cells with enhanced capacity for self-renewal. Glutamine is required to maintain proliferation, viability and self-renewal of ESCs in traditional S/L culture, and restoring anaplerosis with cell-permeable αKG is sufficient to compensate for glutamine withdrawal (Fig. 2a and Supplementary Fig. 2a,b). Therefore, we reasoned that decreased reliance on glutamine anaplerosis would enable cells to better tolerate withdrawal of exogenous glutamine. Indeed, Nanog-high, Nanog-intermediate, and Nanog-low cells were progressively more sensitive to glutamine withdrawal (Supplementary Fig. 2c). Even after several days in culture, "Nanog High" cells were significantly more resistant to apoptosis triggered by glutamine deprivation than their "Nanog Low" counterparts (Fig. 2b and Supplementary Fig. 2d). As a control, we included cells cultured in the presence of 2i, which is sufficient to enable glutamine-independent proliferation[8] and blocked apoptosis induced by glutamine withdrawal (Fig. 2b and Supplementary Fig. 2d). Similarly, while only 40% of control ESCs remained viable after 48 h of glutamine withdrawal, over 60% remained viable in ESCs with constitutive JAK/STAT3 activation (Fig. 2c). Furthermore, cells with enhanced self-renewal mediated by either JAK/STAT3 activation or Klf4/Nanog overexpression were able to increase the number of viable cells in the culture despite the absence of exogenous glutamine (Fig. 2d,e). Conversely, pharmacologic inhibition of JAK/STAT3 signaling sensitized ESCs to glutamine deprivation (Fig. 2f).

In order to determine which metabolic substrates are limiting for survival under conditions of glutamine deprivation, we cultured cells with cell-permeable analogs of pyruvate, αKG and succinate. Only αKG, the direct substrate for de novo glutamine biosynthesis, was capable of rescuing survival and proliferation in the absence of glutamine, and this rescue was contingent upon the ability of cells to use αKG to engage in de novo glutamine biosynthesis (Fig. 2g,h, Supplementary Fig. 2e,f). Therefore, we asked whether cells with enhanced self-renewal are better able to maintain αKG pools during conditions of glutamine withdrawal. In complete medium, even in cells with enhanced self-renewal, glutamine provides the dominant source of carbon for TCA cycle anaplerosis (Fig. 1d,f). Glutamine

withdrawal profoundly reduced steady-state levels of TCA cycle metabolites in all ESC lines tested (Supplementary Fig. 2g,h, Supplementary Table 1). However, both JAK/STAT3-activated and Klf4/Nanog-overexpressing cells were better than their control counterparts at sustaining intracellular pools of αKG, but not downstream TCA cycle metabolites (Supplementary Fig. 2g-j, Supplementary Table 1). As a result, JAK/STAT3 and Klf4/Nanog-overexpressing cells were better able to maintain an elevated αKG/succinate ratio relative to control ESCs in the absence of exogenous glutamine (Fig. 2i,j, Supplementary Table 1).

In addition to serving as an obligate substrate for de novo glutamine biosynthesis, intracellular αKG promotes Nanog expression and increases self-renewal[8,12,14]. Accordingly, while control cells rapidly lost Nanog expression upon glutamine deprivation such that both the overall Nanog expression and the proportion of cells in the Nanog-high population decreased, cells with JAK/STAT3 activation were able to retain Nanog expression and the fraction of cells in the Nanog-high population despite absence of exogenous glutamine (Fig. 2k, Supplementary Fig. 2k). Together, these results indicate that stem cells with strengthened pluripotency networks are not only better able to survive glutamine deprivation but also able to withstand the destabilizing effect of loss of glutamine on markers of self-renewal.

The relative glutamine independence of cells with heightened self-renewal led us to speculate that we could exploit this metabolic property to select for cells with the highest potential for self-renewal. To test this idea, we performed competition assays in which GFP-tracked cells expressing empty vector, Klf4 or Nanog were mixed with parental ESCs and the proportion of GFP+ cells was assessed following 48 h culture in glutamine-replete or glutamine-free medium. Expression of Nanog or Klf4 resulted in a notable selective advantage in the absence of exogenous glutamine, such that the proportion of GFP+ cells increased by 41% (Nanog) or 69% (Klf4) relative to cells cultured in the continuous presence of glutamine (Fig. 2l).

We next asked whether glutamine depletion could select for cells with endogenously strengthened self-renewal potential from within the heterogeneous population characteristic of ESCs. In order to assess population heterogeneity, we developed a quantitative immunofluorescence (IF)-based assay that allowed us to measure the expression levels of pluripotency-associated transcription factors in individual cells. Consistent with previous reports, IF analyses demonstrated that S/L-cultured ESCs exhibit highly variable Nanog expression and relatively homogenous, unimodal Oct4 expression (Supplementary Fig. 3a)[15,32,33]. Addition of 2i increased both homogeneity and overall level of Nanog expression while having minimal effects on mean Oct4 expression (Supplementary Fig. 3a). Of note, 2i eliminated a long tail of “Oct4-low” cells representing approximately 10% of S/L-cultured ESCs that have previously been reported to represent differentiated cells readily apparent in traditional S/L ESC cultures[32] (Supplementary Fig. 3a). As Oct4 is required for pluripotency[34], Oct4-low cells represent the most committed cells within a heterogenous population. Therefore, we asked whether these cells were the most susceptible to glutamine withdrawal. Indeed, within 8 hours of glutamine withdrawal, the proportion of cells in the Oct4-low fraction declined by 50% and 24 h of glutamine deprivation almost entirely

eliminated the population of Oct4-low cells (Fig. 3a). Similarly, 24 h of glutamine deprivation eliminated the majority of Nanog-low cells; however, consistent with the observation that Nanog expression is sensitive to glutamine availability (Fig. 2k), glutamine deprivation also reduced the fraction of cells exhibiting the highest Nanog expression (Supplementary Fig. 3b,c).

Transient withdrawal of exogenous glutamine selects for ESCs with enhanced self-renewal

While Nanog expression is metastable and Nanog-low cells can remain undifferentiated and regenerate Nanog-high cells, cells with very low Oct4 represent differentiated cells that cannot self-renew[32]. As these Oct4-low cells were sensitive to glutamine deprivation, we hypothesized that transient glutamine deprivation would eliminate the most committed cells and thereby improve the overall self-renewal potential of a population. This simple procedure entailed subjecting regularly cultured ESCs to glutamine free medium for 24 h ("pulse") and then recovering the cells in complete medium before seeding for follow-up experiments (Fig. 3b). Immunofluorescence assays confirmed that ESCs subjected to a 24 h period of glutamine withdrawal had higher Nanog and Oct4 on a per-cell basis, reflecting elimination of the most committed cells and the restoration of Nanog levels following glutamine re-addition (Fig. 3c). Similarly, Nanog-GFP reporter cells demonstrated that "pulsed" ESCs were more likely to fall into the Nanog-high population than their conventionally cultured control counterparts (Fig. 3d, Supplementary Fig. 3c). In line with their enhanced expression of pluripotency-associated transcription factors, pulsed cells also exhibited enhanced self-renewal. Colony formation assays analyzed more than one week after the initial pulse demonstrated that pulsed cells were more likely to give rise to undifferentiated colonies and less likely to give rise to differentiated colonies (Fig. 3e,f). Importantly, ESCs subjected to transient glutamine withdrawal remained competent for multi-linage differentiation, giving rise to all three germ layers *in vivo* during teratoma formation (Supplementary Fig. 3d).

We next performed a series of experiments to clarify how transient glutamine withdrawal improves the self-renewal potential of a population of ESCs. We first compared pulsed glutamine withdrawal, which eliminates the most committed cells, with interventions that increase ESC self-renewal. In contrast to pulsed glutamine deprivation, pulsed treatment with 2i or αKG—interventions that transiently increase Nanog-GFP expression (Supplementary Fig. 3e,f)—had no durable effect on the self-renewal capacity of a population of ESC cells (Fig. 3g, Supplementary Fig. 3g). These findings suggest that interventions that increase expression of pluripotency factors may exert different population effects compared to interventions that select against the most committed cells from within a population. To confirm that selective elimination of cells that cannot survive glutamine deprivation is required for the benefit of the pulsed glutamine withdrawal, we supplemented cells with cell-permeable αKG at the time of glutamine withdrawal. Blocking cell death during glutamine deprivation (Fig. 2g) eliminated the selective advantage of glutamine deprivation and abrogated the benefit of the pulse (Fig. 3h). Further supporting the notion that the glutamine withdrawal pulse selects for cells that have the endogenous metabolic capacity to sustain *de novo* glutamine synthesis, inhibition of glutamine synthetase concurrent with glutamine withdrawal eliminated surviving cells and completely blocked the

ability of transient glutamine withdrawal to improve the population self-renewal capacity (Fig. 3h, Supplementary Fig. 3h).

Enhanced self-renewal is associated with the ability to sustain intracellular αKG in the absence of exogenous glutamine (Supplementary Fig. 2i,j). In addition to enabling glutamine synthesis, intracellular αKG can also promote the activity of αKG-dependent chromatin modifying enzymes. The ability of surviving ESCs to preserve intracellular αKG pools to maintain αKG-dependent demethylation reactions may also contribute to the beneficial effect of transient glutamine withdrawal, as addition of the histone H3 trimethylated lysine 27 (H3K27me3) demethylase inhibitor GSK-J4 impaired ESC self-renewal both when administered during transient glutamine withdrawal and in the presence of exogenous glutamine (Supplementary Fig. 3h,i). In contrast to glutamine, glucose is required for the viability of ESCs regardless of self-renewal capacity[8]. Accordingly, pulsed glucose withdrawal strongly reduced the colony-formation capacity of mouse ESCs (Fig. 3i, Supplementary Fig. 3j). Moreover, in line with previous reports that combined glucose and glutamine withdrawal eliminates undifferentiated stem cells[10], pulsed withdrawal of both glucose and glutamine decimated the ability of ESCS to form colonies (Fig. 3i). Together, these findings support a model wherein glutamine deprivation selectively eliminates the most committed cells within a population thereby durably enhancing the overall self-renewal capacity of the remaining cells.

Transient glutamine withdrawal enhances mouse somatic cell reprogramming to pluripotency

Reprogramming of somatic cells to pluripotency represents a major area in which stem cell heterogeneity poses a significant experimental hurdle. Reprogramming is an inefficient process hampered by low efficacy and the persistence of incompletely reprogrammed cells[35]. Interventions that consolidate the pluripotency network enhance reprogramming efficiency: for example, adding 2i to partially reprogrammed cells efficiently promotes the formation of fully reprogrammed cells[36]. Therefore, we tested whether glutamine withdrawal, which selects for cells with strengthened pluripotency gene networks, improves reprogramming efficiency. First, we utilized mouse embryonic fibroblasts (MEFs) harboring a polycistronic cassette enabling doxycycline (dox)-inducible expression of Oct4, Klf4, Sox2 and c-Myc (OKSM) (Fig. 4a)[37]. After eight days of dox-induced OKSM expression, dox removal forces cells to rely on reactivated endogenous pluripotency networks in order to sustain proliferation and ESC-like features including reactivity to alkaline phosphatase (AP). Consequently, cells that were never exposed to dox are fully AP-negative while control cells exposed to dox exhibit heterogeneous AP staining with numerous variably stained regions punctuated with discrete, well-stained colonies reminiscent of undifferentiated ESC colonies (Supplementary Fig. 4a). As expected, sustained 2i treatment over the last four days of reprogramming, which helps cells induce and consolidate pluripotency transcriptional networks[38] and blocks spontaneous differentiation[17], resulted in a marked increase in the number of discrete, ESC-like colonies (Fig. 4b,c). Strikingly, just 24 h of glutamine deprivation two days after dox withdrawal was likewise sufficient to increase the overall number of ESC-like AP+ colonies (Fig. 4b,c). Conversely, there was an overall reduction in flat, intermediately stained regions, consistent with selective elimination of cells with weak

activation of pluripotency-associated gene networks (Fig. 4b). Notably, transient glutamine withdrawal was just as effective at enhancing reprogramming efficiency as transient treatment with 2i (Fig. 4b,c, Supplementary Table 2).

To determine whether glutamine deprivation indeed increased the proportion of cells with activated endogenous pluripotency gene networks, we utilized a second reprogramming system. Here, we infected MEFs harboring a GFP reporter knocked into the endogenous Oct4 locus[39] with viruses carrying dox-inducible OKSM. The Oct4-GFP reporter is helpful in distinguishing fully reprogrammed iPSCs from partially reprogrammed "pre-iPSCs" which, despite having ESC-like morphology, do not activate endogenous pluripotency genes[36] and thus cannot ultimately maintain stable Oct4-GFP expression. Once again, we subjected cells to sustained 2i (7 days) or a 24 h pulse of either glutamine deprivation ("Pulse −Q") or 2i treatment ("Pulse 2i") beginning 2 days after dox withdrawal (Fig. 4d). Consistent with the observation that glutamine withdrawal eliminates the most committed, Oct4-low cells, the number of Oct4-GFP+ cells decreased transiently during glutamine withdrawal but rebounded within 24 h of recovery in glutamine-replete medium (Supplementary Fig. 4b). By the end of the experiment, all interventions significantly increased the proportion of cells expressing Oct4-GFP (Fig. 4e) and increased generation of tight, strongly AP+ ESC-like colonies (Supplementary Fig. 4c). Once again, 24 h of glutamine withdrawal was as effective as 24 h of 2i treatment in enhancing generation of Oct4+iPSCs (Fig. 4e, Supplementary Fig. 4c). Consistent with being fully reprogrammed iPSCs, cells isolated from colonies with compact, ESC-like morphology sustained Oct4-GFP expression for multiple passages in vitro and were able to generate colonies from single cells (Supplemental Fig. 4d,e) while remaining sensitive to LIF withdrawal (Supplemental Fig. 4d,f). These data suggest that transient glutamine deprivation is sufficient to increase the fraction of somatic cells that undergo successful reprogramming and further reveal that a metabolic intervention is as effective as well-described alterations in signal transduction pathways at improving reprogramming efficiency.

Transient glutamine withdrawal increases markers of pluripotency in human ESCs

Finally, we asked whether glutamine withdrawal exerted similar effects in human pluripotent stem cells despite the fact that human ESCs are cultured with dramatically different growth factors and represent a more committed, post-implantation stage of development[40]. As with mouse ESCs, pulsed glutamine withdrawal eliminated a sub-population of cells with low expression of OCT4 (Fig. 4f). Moreover, pulsed glutamine withdrawal resulted in overall enhanced expression of key pluripotency factors SOX2 and OCT4 (Fig. 4f,g). Thus, transient glutamine deprivation represents a general method to enhance expression of key pluripotency markers in both mouse and human pluripotent stem cells under a variety of culture conditions.

Discussion

Here we establish that a distinct metabolic phenotype of naïve mouse embryonic stem cells —reduced reliance on extracellular glutamine as an anaplerotic substrate—is a generalizable feature of cells with enhanced self-renewal. Enhancing ESC self-renewal, either through

manipulation of signal transduction or pluripotency-associated transcription factors, is sufficient to alter cellular metabolism to support enhanced survival in the absence of exogenous glutamine. Conversely, cells with weak pluripotency-associated transcription networks are highly glutamine dependent and rapidly die in the absence of exogenous glutamine supplementation. This association between glutamine dependence and pluripotency offers a potent, non-invasive and reversible method to select for stem cells from a heterogeneous population without altering the biological properties of any individual cell. Recent reports demonstrating potential negative effects of other established methods to enhance ground state pluripotency underscore the potential value of this strategy[41,42]. Moreover, the generalizability of this method to human ESCs, in which the conditions required to achieve the naïve ground state remain a source of continued investigation[43-45], underscores the potential utility of exploiting common metabolic features of cells with enhanced self-renewal. These findings lay the groundwork for future studies to investigate the degree to which glutamine withdrawal affects cells from different lineages and harboring different phenotypes including the potential for self-renewal.

The molecular drivers of reduced glutamine dependence in pluripotent stem cells remain to be fully elucidated. The subtly different effects of the various interventions that increase self-renewal on ESC metabolism may arise as a result of specific transcriptional profiles driven by each intervention or from additional consequences of altered signaling, such as mitochondrial translocation of STAT3[46]. We previously demonstrated that reduced glutamine anaplerosis enables naïve ESCs to maintain high levels of αKG, a critical co-substrate for demethylation reactions that are required to maintain the unique chromatin landscape of naïve ESCs[8,12,14]. This consequence of reduced glutamine oxidation may provide a general advantage for mouse pluripotent stem cells, particularly given that pluripotency transcription factor binding of DNA is highly associated with local DNA demethylation during the establishment of ground state pluripotency[47-49] and that fluctuations in glutamine-derived αKG levels have profound implications for maintenance of pluripotency[12,14]. However, decreased glutamine anaplerosis may provide additional advantages to naïve ESCs, independent of αKG. The ability to oxidize either glucose or glutamine to maintain energy homeostasis may be of particular value under conditions when either glucose or glutamine becomes limiting[50,51]. Furthermore, decreased glutamine anaplerosis may facilitate the utilization of glutamine for other purposes, including glutamate-dependent uptake of non-essential amino acids[52] as well as nucleotide biosynthesis[53]. Finally, glutamine not used as an anaplerotic substrate can be utilized for the synthesis of glutathione, which is essential to prevent cysteine oxidation and degradation of Oct4 in human ESCs[54].

Prior studies have identified selective nutrient dependencies that can be exploited to preferentially eliminate ESCs from a population[55]. Our findings offer a strategy for the preferential enrichment of highly self-renewing, pluripotent ESCs. These results add to an increasing body of work supporting the idea that individual cell types may engage in distinct modes of nutrient utilization to support diverse cell fate decisions, including proliferation as well as regulation of gene expression. Further study of the specialized metabolism of individual cell types may deepen our understanding of how nutrient availability can affect

cell fate decisions *in vivo* and provide further opportunities for intervention to select for cells with desired phenotypes.

Methods

Cell Culture.

Mouse ESC lines (ESC-1, ESC-2) were previously generated from C57BL/6 × 129S4/SvJae F1 male embryos[8]. Nanog-GFP reporter ESCs were a gift from R. Jaenisch (MIT). Nanog-GFP lines expressing the chimeric LIF receptor (a gift from A. Smith)[21] and ESC-1 lines overexpressing Nanog or Klf4 were previously generated[56]. ESC-1 cells were used for all experiments unless otherwise noted. ESCs were maintained on gelatin-coated plates in serum/LIF (S/L) medium containing Knockout DMEM (Life 10829–018) supplemented with 10% FBS (Gemini), 0.1 mM 2-mercaptoethanol, 2 mM L-glutamine and 1000 U/mL LIF (Gemini). For culture in 2i (S/L+2i), S/L medium was supplemented with 3 μM CHIR99021 (Stemgent) and 1 μM PD0325901 (Stemgent). Cells were adapted to 2i or GCSF (Gemini) by passaging cells in S/L+2i or S/L+GCSF medium at least three times prior to use in experiments. S/L+2i-adapted cells were maintained for a maximum of nine passages. All cells were routinely tested for mycoplasma. For human embryonic stem cells (hESC) culture, an H1 hESC line (NIHhESC-10–0043) with an inducible Cas9 insertion was used[57]. This line was maintained in chemically defined, serum-free E8 conditions (Thermo Fisher Scientific, A1517001) on tissue culture treated polystyrene plates coated with vitronectin (Thermo Fisher Scientific, A14700). hESCs were split with 0.5mM EDTA at a 1:10–1:20 split ratio every 3–5 days. Cells have been confirmed to be mycoplasma-free by the MSKCC Antibody and Bioresource Core Facility. All experiments were approved by the Tri-SCI Embryonic Stem Cell Research Oversight Committee (ESCRO). Further details on cell lines can be found in the Reporting Summary.

Nutrient deprivation experiments.

For glutamine deprivation experiments in mouse ESCs, cells were initially plated in standard S/L medium as described above. The following day, cells were washed with PBS and then cultured in experimental medium containing a 1:1 mix of glutamine-free DMEM (Gibco 11960–051) and glutamine-free Neurobasal medium (Gibco 21103–049) including 10% dialyzed FBS, 2-mercaptoethanol, and LIF as described above and containing (“+Q”) or lacking (“−Q”) L-glutamine (2 mM) as indicated. When indicated, dimethyl-α-ketoglutarate (Sigma 349631) dissolved in DMSO to 1 M was added to a final concentration of 4 mM. For glucose and glutamine deprivation experiments, cells were cultured in medium containing a 1:1 mix of glutamine and glucose-free DMEM (Gibco A14430–01) and glutamine and glucose-free Neurobasal-A medium (Gibco A24775–01) including 10% dialyzed FBS and all supplements as described above and containing or lacking glucose or glutamine as indicated.

Embryonic stem cell competition assays.

GFP-negative parental ESCs were mixed with GFP-positive vector or Klf4/Nanog-overexpressing transgenic ESCs and seeded at a concentration of 30,000 total cells per well of a 12-well plate in triplicate. The following day, cells were washed with PBS and then

changed to experimental medium containing a 1:1 mix of glutamine-free DMEM and glutamine-free Neurobasal medium including 10% dialyzed FBS, 2-mercaptoethanol, LIF, and containing ("+Q") or lacking ("−Q") L-glutamine as indicated. After 48 h, cells were trypsinized for flow cytometry analysis. Cells were evaluated for GFP and DAPI on either a LSRFortessa or LSR-II machine (Becton Dickinson). Analysis of DAPI exclusion and GFP mean fluorescence intensity was performed using FlowJo v9.0.

Glutamine pulse experiments.

For transient glutamine withdrawal ("pulse") experiments, cells were initially plated in standard S/L medium as described above. The following day, cells were washed with PBS and then changed to experimental medium containing a 1:1 mix of glutamine-free DMEM and glutamine-free Neurobasal medium including 10% dialyzed FBS, 2-mercaptoethanol, LIF, and containing ("Ctrl") or lacking ("Pulse −Q") L-glutamine as indicated. 24 h later, cells were washed with PBS and then returned to glutamine-replete medium ("Recover"). 24 h later, cells were subjected to either image analysis, flow cytometry, or plated for colony formation assays as indicated. For glutamine pulse experiments in human ESCs, cells were initially plated at a density of 300,000 cells/well in a tissue-culture treated polystyrene 12-well plate coated with vitronectin (Thermo Fisher Scientific, A14700) in E8 medium (Thermo Fisher Scientific, A1517001) containing 10 μM ROCK inhibitor Y-27632 (Selleck Chemicals S1049). 24 h after plating, medium was changed to modified E8 medium containing: DMEM high glucose without glutamine (Thermo Fisher 11960044), 10.7 mg/L Transferrin (Sigma T0665), 64 mg/L L-Ascorbic Acid (Sigma A890), 14 μg/L Sodium Selenite (Sigma S5261), 543 mg/L Sodium Bicarbonate (Research Products International 144558), 19.4 mg/L insulin (Sigma I9278), 100 μg/L bFGF (EMD Millipore GF003AF), 2 μg/L TGFβ1 (Peprotech 10021), and 2 mM L-glutamine. After 24 h of culture in modified E8 medium, medium was changed to modified E8 medium containing 2 mM or 0 mM L-glutamine for 24 h. All cells were then changed to modified E8 medium containing 2 mM L-glutamine and cultured for 24 h before harvest for analysis.

Growth curves.

ESCs were seeded at a density of 30,000–40,000 cells per well of a 12-well plate. The following day, three wells of each line were counted to determine the starting cell number. The remaining cells were washed with PBS and cultured in medium containing a 1:1 mix of glutamine-free DMEM and glutamine-free Neurobasal medium including 10% dialyzed FBS, 2-mercaptoethanol, LIF, and containing or lacking L-glutamine or glucose as indicated and with or without the addition of supplements as indicated: dimethyl-α-ketoglutarate (4 mM), dimethyl-succinate (4 mM), methyl-pyruvate (2 mM), ruxolitinib (500 nM), methionine sulfoximine (1 mM). Cells were counted on the indicated days thereafter using a Beckman Multisizer 4e with a cell volume gate of 400 – 10,000 fL. Cell counts were normalized to starting cell number. All curves were performed at least two independent times.

Colony formation assays.

Cells were seeded at 200 or 500 cells per well in six-well plates in standard S/L medium. Medium was refreshed every 2–3 days. Six to seven days after initial seeding, wells were

fixed with citrate/acetone/3% formaldehyde for 30 seconds and stained using the Leukocyte Alkaline Phosphatase Kit (Sigma) according to manufacturer instructions. Colonies were scored manually by two independent reviewers.

Fluorescence activated cell sorting.

For evaluation of cell viability and Nanog-GFP expression, Nanog-GFP ESCs[30] were seeded at a concentration of 40,000 cells per well of a 12-well plate. The next day, cells were washed with PBS and medium was changed to experimental medium containing a 1:1 mix of glutamine-free DMEM and glutamine-free Neurobasal medium including 10% dialyzed FBS, 2-mercaptoethanol, LIF, and containing ("+Q") or lacking ("−Q") L-glutamine as indicated. On the day of analysis, cells were trypsinized and resuspended in FACS buffer (PBS + 2% FBS + 1 mM EDTA) containing DAPI (1 μg/mL). Cells were evaluated for GFP and DAPI on either a LSRFortessa or LSR-II machine and FACSDiva software (Beckman Dickinson). Viable cells were those excluding DAPI (100-fold less than DAPI-positive cells). Nanog-GFP expression was measured by GFP mean fluorescence intensity and quantified using FlowJo v9.0. All experiments were performed at least two independent times.

For sorting of Nanog High, Nanog Medium, and Nanog Low populations, Nanog-GFP ESCs that were cultured either in S/L medium or adapted to S/L+2i medium as described above were resuspended in sterile FACS buffer containing DAPI. DAPI-excluding cells were evaluated for Nanog-GFP expression on a BD FACSAria III cell sorter (Becton Dickinson). "Nanog High," "Nanog Medium," and "Nanog Low" populations were sorted based on Nanog-GFP expression levels in the highest 10%, median 10%, and lowest 10% of the population, respectively. Following sorting, cells were washed 2 times with PBS to remove any residual FACS buffer and plated in 6-well gelatin-coated plates in standard S/L medium with the addition of penicillin/streptomycin (Life technologies). Cells were used 24 to 72 h later for experiments.

Evaluation of apoptosis was performed using an Annexin V Apoptosis Detection kit (BD Biosciences BDB556570). Nanog-GFP ESCs that had been sorted based on Nanog-GFP expression 24 h earlier as described above were plated in standard S/L medium. The next day, cells were washed with PBS and cultured in experimental medium containing a 1:1 mix of glutamine-free DMEM and glutamine-free Neurobasal medium including 10% dialyzed FBS, 2-mercaptoethanol, LIF, and containing ("+Q") or lacking ("−Q") L-glutamine as indicated. 24 h later, cells were trypsinized and resuspended in Annexin V binding buffer containing FITC-conjugated Annexin V and propidium iodide (PI) for 15 min at room temperature. Subsequently, excess binding buffer was added and both FITC and PI fluorescence was assessed on an LSRFortessa machine (Becton Dickinson). Apoptosis was quantified as cells positive for Annexin V based on a 100-fold increase in fluorescence as compared to negative cells.

For evaluation of OCT4 and SOX2 expression in human ESCs, cells were dissociated using TryPLE-Select (Thermo Fisher 12563029) and resuspended in FACS buffer (5% FBS and 5 mM EDTA in FBS). Cells were first stained with LIVE/DEAD Violet (Molecular Probe, L34955, 1:1,000) for 30 min at room temperature. Cells were fixed and permeabilized in 1X

fix/perm buffer (eBioscience, 00–5523-00) for 1 h at room temperature. Cells were then stained with fluorophore conjugated antibodies OCT4-APC (eBioscience 50–5841- 82, 1:25) and SOX2-Alexa488 (eBioscience 53–9811-82, 1:100) in permeabilization buffer (Thermo Fisher 00–8333-56) for 30 min at room temperature. Cells were washed by addition of FACS buffer and centrifugation between all steps. Analysis was performed after resuspension in FACS buffer using an LSRFortessa machine (Becton Dickinson).

Further details on flow cytometry can be found in the Reporting Summary.

Metabolic analyses.

For steady state TCA cycle metabolite measurements, cells were seeded in standard S/L medium in 6-well plates. 24 h later, cells were washed with PBS and changed into experimental medium containing a 1:1 mix of glutamine-free DMEM and glutamine-free Neurobasal medium including 10% dialyzed FBS, 2-mercaptoethanol, LIF, and 2 mM L-glutamine. The next day, cells were washed with PBS and subjected to the same experimental medium either with or without 2 mM glutamine. 8 h later, metabolites were extracted with 1 mL ice-cold 80% methanol containing 2 μM deuterated 2-hydroxyglutarate (D-2-hydroxyglutaric-2,3,3,4,4-d_5 acid, d5–2HG) as an internal standard. After overnight incubation at −80°C, lysates were harvested and centrifuged at 21,000*g* for 20 minutes to remove protein. Extracts were dried in an evaporator (Genevac EZ-2 Elite) and resuspended by incubating at 30°C for 2 h in 50 μL of 40 mg/mL methoxyamine hydrochloride in pyridine. Metabolites were further derivatized by addition of 80 μL of MSTFA + 1% TCMS (Thermo Scientific) and 70 μl ethyl acetate (Sigma) and then incubated at 37°C for 30 min. Samples were analyzed using an Agilent 7890A GC coupled to Agilent 5977C mass selective detector. The GC was operated in splitless mode with constant helium gas flow at 1 mL/min. 1 μl of derivatized metabolites was injected onto an HP-5MS column and the GC oven temperature ramped from 60°C to 290°C over 25 minutes. Peaks representing compounds of interest were extracted and integrated using MassHunter software (Agilent Technologies) and then normalized to both the internal standard (d5–2HG) peak area and protein content of duplicate samples as determined by BCA protein assay (Thermo Scientific). Ions used for quantification of metabolite levels are as follows: d5–2HG *m/z* 354; αKG, *m/z* 304; aspartate, *m/z* 334; citrate, *m/z* 465; fumarate, *m/z* 245; glutamate, *m/z* 363; malate, *m/z* 335 and succinate, *m/z* 247. All peaks were manually inspected and verified relative to known spectra for each metabolite.

For isotope tracing studies, cells were seeded in standard S/L medium in 6-well plates. 24 h later, cells were washed with PBS and changed into experimental medium containing a 1:1 mix of glutamine-free DMEM and glutamine-free Neurobasal medium including 10% dialyzed FBS, 2-mercaptoethanol, LIF, and 2 mM L-glutamine. The next day, cells were washed with PBS and changed into medium containing a 1:1 combination of glucose- and glutamine-free DMEM (Gibco) and glucose- and glutamine-free Neurobasal-A medium (ThermoFisher A24775–01) supplemented with ^{12}C-glucose (Sigma) and ^{12}C-glutamine (Gibco) or the ^{13}C versions of each metabolite, [U-^{13}C]glucose or [U-^{13}C]glutamine (Cambridge Isotope Labs) to a final concentration of 20 mM (glucose) and 2 mM (glutamine) for 4 h. Enrichment of ^{13}C was assessed by quantifying the abundance of the

following ions: αKG, *m/z* 304–318; aspartate, *m/z* 334–346; citrate, *m/z* 465–482; fumarate, *m/z* 245–254; glutamate, *m/z* 363–377 and malate, *m/z* 335–347. Correction for natural isotope abundance was performed using IsoCor software[58].

Immunofluorescence and microscopy.

For mouse ESCs, cells were seeded on 12-well MatTek glass-bottom dishes (P12G-1.0–10-F*) coated in laminin (Sigma, 10 μg/mL in PBS containing Ca^{2+} and Mg^{2+}). Cells were fixed in 2% paraformaldehyde for 10 min and then permeabilized in 0.1% tween. Cells were washed with PBS and blocked for 1 h in 2.5% BSA in PBS. After blocking, cells were incubated overnight with primary antibodies diluted in blocking solution. The following antibodies were used: Oct¾ (Santa Cruz Biotechnologies, sc-5279 at 1:100) and Nanog (eBioscience, 145761–80 at 1:125). The next day, cells were washed with PBS and incubated with secondary antibodies (AlexaFluor 488 or 594 or 647, Molecular Probes) diluted 1:500 in blocking solution for 1 h. For nuclear counterstaining, Hoechst 33342 (Molecular Probes, H3570 at 1 μg/mL) was added to the same secondary solution. After washing with PBS, cells were stored in the dark and imaged within 1 or 2 days. Cells were imaged using an AxioObserver.Z1 epifluorescence inverted microscope with a motorized stage. A CCD attached camera allowed digital image acquisition (Hammamatsu, Orca II). For multi-well and multidimensional microscopy, definite focus was used and the microscope was programmed to image consecutive image fields (typically 60 per condition). These fields were stitched together using the built-in Axiovision function and exported as raw 16-bit TIFF files without further processing. Typically at least 10,000 cells per well at 200x magnification were imaged.

Image analysis required three steps: cell detection, nuclear segmentation and fluorescence detection in a per cell basis. These steps were implemented on custom-made Matlab (MathWorks) routines. First, cells were detected by adapting a Matlab implementation of the IDL particle tracking code developed by David Grier, John Crocker, and Eric Weeks (http://physics.georgetown.edu/matlab/). This algorithm finds cells as peaks in a Fourier space rather than by thresholding. This approach is less susceptible to problems that typically arise when segmenting large images such as autofluorescent and bright speckles or day-to-day variability in imaging conditions. Cell detection allowed us to count, identify and get the spatial coordinates (centroid) for each cell. Second, nuclear segmentation was achieved by a combination of regular thresholding together with a watershed process based on the distance of cell centroids determined in the previous step. Obtained nuclear regions were then used as masks to quantify pixel intensities for all the fluorescent channels (that reported levels of different proteins) on a per cell basis. We used cumulative values, which were then normalized to the Hoechst staining to correct for area, cell location along the Z-axis and DNA condensation differences. After image analysis, data was processed and plotted also with Matlab. Raw data, image analysis, and data processing routines are available upon request. Further details on staining and analysis can be found in the Reporting Summary.

Quantification of gene expression.

RNA was isolated from six-well plates using Trizol (Invitrogen) according to manufacturer instructions. 200 ng RNA was used for cDNA synthesis using iScript (BioRad). Quantitative real-time PCR analysis was performed in technical triplicate using QuantStudio 7 Flex (Applied Biosystems) with Power SYBR Green (Life Technologies). All data were generated using cDNA from triplicate wells for each condition. *Actin* was used as an endogenous control for all experiments. The following primers were used: *Actin*, forward, 5'- GCTCTTTTCCAGCCTTCCTT-3', reverse, 5'- CTTCTGCATCCTGTCAGCAA −3'; *Nanog*, forward, 5'-AAGATGCGGACTGTGTTCTC-3', reverse, 5'-CGCTTGCACTTCATCCTTTG-3'; *Stat3*, forward, 5'-GTCCTTTTCCACCCAAGTGA-3', reverse, 5'-TATCTTGGCCCTTTGGAATG-3'; *Tfcp2l1*, forward, 5'-GGGGACTACTCGGAGCATCT-3', reverse, 5'-TTCCGATCAGCTCCCTTG-3'; *Esrrb*, forward, 5'- AACAGCCCCTACCTGAACCT-3', reverse, 5'-TGCCAATTCACAGAGAGTGG −3'; *Klf4*, forward, 5'-CGGGAAGGGAGAAGACACT-3', reverse, 5'-GAGTTCCTCACGCCAACG-3'; *Zfp42*, forward, 5'-TCCATGGCATAGTTCCAACAG-3', reverse, 5'-TAACTGATTTTCTGCCGTATGC-3'; *Fgf5*, forward, 5'-AAACTCCATGCAAGTGCCAAAT-3', reverse, 5'-TCTCGGCCTGTCTTTTCAGTTC-3'.

Western blotting

Protein lysates were extracted in 1X RIPA buffer (Cell Signaling Technology), separated by SDS–PAGE and transferred to nitrocellulose membranes (Bio-Rad). Membranes were blocked in 3% milk in Tris-buffered saline with 0.1% Tween-20 (TBST) and incubated at 4 °C with primary antibodies overnight. After TBST washes the next day, membranes were incubated with horseradish peroxidase-conjugated secondary antibodies for 2 h, incubated with ECL (Thermo Scientific) and imaged using an SRX-101A X-Ray Film Processor (Konica Minolta). Antibodies used (at 1:1,000 unless otherwise noted) were: Nanog (AF2729, R&D Systems), Klf4 (ab129473, Abcam), phospho-Stat3 (9138, Cell Signaling Technology), Stat3 (9139, Cell Signaling Technology), and Tubulin (1:10,000, T9026, Sigma).

Reprogramming of mouse embryonic fibroblasts to induced pluripotent stem cells.

For assessment of colony formation, Collagen-OKSM MEFs which contain an optimized reverse tetracycline-dependent transactivator (M2-rtTA) targeted to the constitutively active *Rosa26* locus (https://www.jax.org/strain/006965) and a polycistronic cassette encoding Oct4, Klf4, Sox2, and c-Myc targeted to the *Col1a1* locus under control of a tetracycline-dependent minimal promoter (tetOP)[37] were plated 10,000 cells per plate on gelatin-coated 6-well plates. 24 h later, cells were washed with PBS and changed to S/L medium containing 1 μg/mL of doxycycline. Medium was replaced every 2 days. After 8 days of culture in S/L medium containing doxycycline, cells were washed with PBS and changed into experimental medium containing a 1:1 mix of glutamine-free DMEM and glutamine-free Neurobasal medium including 10% dialyzed FBS, 2-mercaptoethanol, LIF, and 2 mM L-

glutamine without doxycycline. On day 10, all cells were washed with PBS and changed into experimental medium containing 2 mM L-glutamine ("Ctrl"), no glutamine ("Pulse −Q") or 2 mM L-glutamine plus 3 μM CHIR99021 (Stemgent) and 1 μM PD0325901 (Stemgent) ("2i" and "Pulse 2i"). 24 h later, all cells were washed with PBS and returned to experimental medium containing 2 mM L-glutamine. "2i continuous" treated samples were supplemented with 2i from day 10 for the duration of the experiment. After 14 days, cells were stained for alkaline phosphatase expression and manually scored for colony formation.

For assessment of Oct4-GFP expression, MEFs containing a GFP allele targeted to the endogenous *Oct4/Pou5f1* locus (https://www.jax.org/strain/008214)[59] were plated at 20,000 cells per well on gelatin-coated 6-well plates in DMEM medium containing 10% FBS. 24 h later, cells were infected with lentivirus containing Oct4, Sox2, Klf4, and c-Myc under control of the tetracycline operator and a minimal CMV promoter (a gift from R. Jaenisch, Whitehead Institute, Addgene plasmid #20321). 24 h after infection, plates were washed with PBS and changed to standard S/L medium containing 1 μg/mL of doxycycline. Medium was replaced every 2 days. After 12 days of culture in S/L medium containing doxycycline, cells were washed with PBS and changed into experimental medium containing a 1:1 mix of glutamine-free DMEM and glutamine-free Neurobasal medium including 10% dialyzed FBS, 2-mercaptoethanol, LIF, and 2 mM L-glutamine without doxycycline. On day 14, all cells were washed with PBS and changed into experimental medium containing 2 mM L-glutamine ("Ctrl"), no glutamine ("Pulse −Q") or 2 mM L-glutamine plus 3 μM CHIR99021 (Stemgent) and 1 μM PD0325901 (Stemgent) ("2i", "Pulse 2i"). 24 h later, all cells were washed with PBS and returned to experimental medium containing 2 mM L-glutamine. "2i continuous" treated samples were supplemented with 2i from day 14 for the duration of the experiment. On day 20 or other days as indicated, cells were trypsinized, resuspended in FACS buffer containing DAPI and assessed for GFP expression by flow cytometry as described above. Oct4-GFP positivity was defined by expression of GFP at least 10-fold higher than that of negative cells.

Teratomas.

ESCs were initially plated in standard S/L medium as described above. The following day, cells were washed with PBS and then changed to experimental medium containing a 1:1 mix of glutamine-free DMEM and glutamine-free Neurobasal medium including 10% dialyzed FBS, 2-mercaptoethanol, LIF, and containing ("Ctrl") or lacking ("Pulse −Q") L-glutamine as indicated. 24 h later, cells were washed with PBS and then returned to glutamine-replete medium ("Recover"). 24 h later, 1×10^6 cells per replicate were harvested from each group and mixed 1:1 with medium plus Matrigel Basement Membrane Matrix (BD) and injected into the flanks of recipient female SCID littermate mice aged 8–12 weeks (NOD *scid* gamma JAX 005557 purchased from Jackson Laboratories). All conditions produced tumors in 4–8 weeks. Mice were euthanized before tumor size exceeded 1.5 cm in diameter. Tumors were excised and fixed in 4% paraformaldehyde overnight at 4 °C. Tumors were paraffin-embedded and sections were stained with haematoxylin and eosin according to standard procedures by HistoWiz. All experiments were performed in accordance with a protocol approved by the Memorial Sloan Kettering Institutional Animal Care and Use Committee.

Statistical analyses.

GraphPad PRISM 7 software was used for statistical analyses except for IF data. Error bars, *P* values and statistical tests are reported in figure legends. Statistical analyses on images were performed using Matlab. We set the threshold to define "Oct4-low" cells as one standard deviation below the mean values of the control population (typically S/L in the presence of glutamine).

Data Availability.

The data and MatLab code that support the findings of this study are available from the corresponding author upon reasonable request. Source data for all GC-MS data are provided in Supplementary Table 1.

Supplementary Material

Refer to Web version on PubMed Central for supplementary material.

Acknowledgments

We thank the Finley lab for discussion and A. Intlekofer for critical feedback. We thank A. Smith (University of Cambridge) for the gift of the chimeric LIF receptor and R. Jaenisch (Whitehead Institute for Biomedical Research) for the gift of the Nanog-GFP ESCs. S.A.V. is a Parker Fellow with the Parker Institute of Cancer Immunotherapy. B.P.R was supported by an NIH T32 Training Grant in Molecular and Cellular Biology (T32GM008539). L.W.S.F. is a Searle Scholar and was a Dale F. Frey-William Raveis Charitable Fund Scientist supported by the Damon Runyon Cancer Research Foundation (DFS-23–17). This work was additionally supported by The Concern Foundation and The Anna Fuller Fund (to L.W.S.F.), The Starr Foundation (I11–0039 to L.W.S.F.), a Pathway to Independence Award from NIH (R00 CA191021 to C.C.-F.), NIH/NIDDK (R01DK096239 to D.H.), and the Memorial Sloan Kettering Cancer Center Support Grant P30 CA008748.

References

1. DeBerardinis RJ, Lum JJ, Hatzivassiliou G & Thompson CB The biology of cancer: metabolic reprogramming fuels cell growth and proliferation. Cell metabolism 7, 11–20, doi:10.1016/j.cmet.2007.10.002 (2008). [PubMed: 18177721]
2. Palm W & Thompson CB Nutrient acquisition strategies of mammalian cells. Nature 546, 234–242, doi:10.1038/nature22379 (2017). [PubMed: 28593971]
3. Vander Heiden MG & DeBerardinis RJ Understanding the Intersections between Metabolism and Cancer Biology. Cell 168, 657–669, doi:10.1016/j.cell.2016.12.039 (2017). [PubMed: 28187287]
4. Schvartzman JM, Thompson CB & Finley LWS Metabolic regulation of chromatin modifications and gene expression. The Journal of cell biology 217, 2247–2259, doi:10.1083/jcb.201803061 (2018). [PubMed: 29760106]
5. Saxton RA & Sabatini DM mTOR Signaling in Growth, Metabolism, and Disease. Cell 168, 960–976, doi:10.1016/j.cell.2017.02.004 (2017). [PubMed: 28283069]
6. Su X, Wellen KE & Rabinowitz JD Metabolic control of methylation and acetylation. Curr Opin Chem Biol 30, 52–60, doi:10.1016/j.cbpa.2015.10.030 (2016). [PubMed: 26629854]
7. Lu C & Thompson CB Metabolic regulation of epigenetics. Cell metabolism 16, 9–17, doi:10.1016/j.cmet.2012.06.001 (2012). [PubMed: 22768835]
8. Carey BW, Finley LW, Cross JR, Allis CD & Thompson CB Intracellular alpha-ketoglutarate maintains the pluripotency of embryonic stem cells. Nature 518, 413–416, doi:10.1038/nature13981 (2015). [PubMed: 25487152]
9. Gu W et al. Glycolytic Metabolism Plays a Functional Role in Regulating Human Pluripotent Stem Cell State. Cell stem cell 19, 476–490, doi:10.1016/j.stem.2016.08.008 (2016). [PubMed: 27618217]

10. Tohyama S et al. Glutamine Oxidation Is Indispensable for Survival of Human Pluripotent Stem Cells. Cell metabolism 23, 663–674, doi:10.1016/j.cmet.2016.03.001 (2016). [PubMed: 27050306]
11. Zhang H et al. Distinct Metabolic States Can Support Self-Renewal and Lipogenesis in Human Pluripotent Stem Cells under Different Culture Conditions. Cell Rep 16, 1536–1547, doi:10.1016/j.celrep.2016.06.102 (2016). [PubMed: 27477285]
12. Hwang IY et al. Psat1-Dependent Fluctuations in alpha-Ketoglutarate Affect the Timing of ESC Differentiation. Cell metabolism 24, 494–501, doi:10.1016/j.cmet.2016.06.014 (2016). [PubMed: 27476977]
13. Moussaieff A et al. Glycolysis-mediated changes in acetyl-CoA and histone acetylation control the early differentiation of embryonic stem cells. Cell metabolism 21, 392–402, doi:10.1016/j.cmet.2015.02.002 (2015). [PubMed: 25738455]
14. TeSlaa T et al. alpha-Ketoglutarate Accelerates the Initial Differentiation of Primed Human Pluripotent Stem Cells. Cell metabolism 24, 485–493, doi:10.1016/j.cmet.2016.07.002 (2016). [PubMed: 27476976]
15. Chambers I et al. Nanog safeguards pluripotency and mediates germline development. Nature 450, 1230–1234, doi:10.1038/nature06403 (2007). [PubMed: 18097409]
16. Filipczyk A et al. Biallelic expression of nanog protein in mouse embryonic stem cells. Cell Stem Cell 13, 12–13, doi:10.1016/j.stem.2013.04.025 (2013). [PubMed: 23827706]
17. Ying QL et al. The ground state of embryonic stem cell self-renewal. Nature 453, 519–523, doi:10.1038/nature06968 (2008). [PubMed: 18497825]
18. Chisolm DA et al. CCCTC-Binding Factor Translates Interleukin 2- and alpha-Ketoglutarate-Sensitive Metabolic Changes in T Cells into Context-Dependent Gene Programs. Immunity 47, 251–267 e257, doi:10.1016/j.immuni.2017.07.015 (2017). [PubMed: 28813658]
19. Liu PS et al. alpha-ketoglutarate orchestrates macrophage activation through metabolic and epigenetic reprogramming. Nat Immunol 18, 985–994, doi:10.1038/ni.3796 (2017). [PubMed: 28714978]
20. Yang Q et al. AMPK/alpha-Ketoglutarate Axis Dynamically Mediates DNA Demethylation in the Prdm16 Promoter and Brown Adipogenesis. Cell Metab 24, 542–554, doi:10.1016/j.cmet.2016.08.010 (2016). [PubMed: 27641099]
21. Burdon T, Stracey C, Chambers I, Nichols J & Smith A Suppression of SHP-2 and ERK signalling promotes self-renewal of mouse embryonic stem cells. Dev Biol 210, 30–43, doi:10.1006/dbio.1999.9265 (1999). [PubMed: 10364425]
22. van Oosten AL, Costa Y, Smith A & Silva JC JAK/STAT3 signalling is sufficient and dominant over antagonistic cues for the establishment of naive pluripotency. Nature communications 3, 817, doi:10.1038/ncomms1822 (2012).
23. Martello G, Bertone P & Smith A Identification of the missing pluripotency mediator downstream of leukaemia inhibitory factor. EMBO J 32, 2561–2574, doi:10.1038/emboj.2013.177 (2013). [PubMed: 23942233]
24. Chambers I et al. Functional expression cloning of Nanog, a pluripotency sustaining factor in embryonic stem cells. Cell 113, 643–655 (2003). [PubMed: 12787505]
25. Mitsui K et al. The homeoprotein Nanog is required for maintenance of pluripotency in mouse epiblast and ES cells. Cell 113, 631–642 (2003). [PubMed: 12787504]
26. Zhang P, Andrianakos R, Yang Y, Liu C & Lu W Kruppel-like factor 4 (Klf4) prevents embryonic stem (ES) cell differentiation by regulating Nanog gene expression. J Biol Chem 285, 9180–9189, doi:10.1074/jbc.M109.077958 (2010). [PubMed: 20071344]
27. Festuccia N et al. Esrrb is a direct Nanog target gene that can substitute for Nanog function in pluripotent cells. Cell stem cell 11, 477–490, doi:10.1016/j.stem.2012.08.002 (2012). [PubMed: 23040477]
28. Shi W et al. Regulation of the pluripotency marker Rex-1 by Nanog and Sox2. The Journal of biological chemistry 281, 23319–23325, doi:10.1074/jbc.M601811200 (2006). [PubMed: 16714766]

29. Cheng T et al. Pyruvate carboxylase is required for glutamine-independent growth of tumor cells. Proceedings of the National Academy of Sciences of the United States of America 108, 8674–8679, doi:10.1073/pnas.1016627108 (2011). [PubMed: 21555572]
30. Faddah DA et al. Single-cell analysis reveals that expression of nanog is biallelic and equally variable as that of other pluripotency factors in mouse ESCs. Cell stem cell 13, 23–29, doi:10.1016/j.stem.2013.04.019 (2013). [PubMed: 23827708]
31. Boroviak T, Loos R, Bertone P, Smith A & Nichols J The ability of inner-cell-mass cells to self-renew as embryonic stem cells is acquired following epiblast specification. Nat Cell Biol 16, 516–528, doi:10.1038/ncb2965 (2014). [PubMed: 24859004]
32. Karwacki-Neisius V et al. Reduced Oct4 expression directs a robust pluripotent state with distinct signaling activity and increased enhancer occupancy by Oct4 and Nanog. Cell Stem Cell 12, 531–545, doi:10.1016/j.stem.2013.04.023 (2013). [PubMed: 23642364]
33. Silva J et al. Nanog is the gateway to the pluripotent ground state. Cell 138, 722–737, doi:10.1016/j.cell.2009.07.039 (2009). [PubMed: 19703398]
34. Nichols J et al. Formation of pluripotent stem cells in the mammalian embryo depends on the POU transcription factor Oct4. Cell 95, 379–391 (1998). [PubMed: 9814708]
35. Hochedlinger K & Jaenisch R Induced Pluripotency and Epigenetic Reprogramming. Cold Spring Harb Perspect Biol 7, doi:10.1101/cshperspect.a019448 (2015).
36. Silva J et al. Promotion of reprogramming to ground state pluripotency by signal inhibition. PLoS Biol 6, e253, doi:10.1371/journal.pbio.0060253 (2008). [PubMed: 18942890]
37. Stadtfeld M, Maherali N, Borkent M & Hochedlinger K A reprogrammable mouse strain from gene-targeted embryonic stem cells. Nat Methods 7, 53–55, doi:10.1038/nmeth.1409 (2010). [PubMed: 20010832]
38. Dunn SJ, Martello G, Yordanov B, Emmott S & Smith AG Defining an essential transcription factor program for naive pluripotency. Science 344, 1156–1160, doi:10.1126/science.1248882 (2014). [PubMed: 24904165]
39. Buganim Y et al. The developmental potential of iPSCs is greatly influenced by reprogramming factor selection. Cell Stem Cell 15, 295–309, doi:10.1016/j.stem.2014.07.003 (2014). [PubMed: 25192464]
40. Weinberger L, Ayyash M, Novershtern N & Hanna JH Dynamic stem cell states: naive to primed pluripotency in rodents and humans. Nature reviews. Molecular cell biology 17, 155–169, doi:10.1038/nrm.2015.28 (2016). [PubMed: 26860365]
41. Choi J et al. Prolonged Mek½ suppression impairs the developmental potential of embryonic stem cells. Nature 548, 219–223, doi:10.1038/nature23274 (2017). [PubMed: 28746311]
42. Yagi M et al. Derivation of ground-state female ES cells maintaining gamete-derived DNA methylation. Nature 548, 224–227, doi:10.1038/nature23286 (2017). [PubMed: 28746308]
43. Huang K, Maruyama T & Fan G The naive state of human pluripotent stem cells: a synthesis of stem cell and preimplantation embryo transcriptome analyses. Cell stem cell 15, 410–415, doi:10.1016/j.stem.2014.09.014 (2014). [PubMed: 25280217]
44. Wang J et al. Isolation and cultivation of naive-like human pluripotent stem cells based on HERVH expression. Nature protocols 11, 327–346, doi:10.1038/nprot.2016.016 (2016). [PubMed: 26797457]
45. Warrier S et al. Direct comparison of distinct naive pluripotent states in human embryonic stem cells. Nature communications 8, 15055, doi:10.1038/ncomms15055 (2017).
46. Carbognin E, Betto RM, Soriano ME, Smith AG & Martello G Stat3 promotes mitochondrial transcription and oxidative respiration during maintenance and induction of naive pluripotency. EMBO J 35, 618–634, doi:10.15252/embj.201592629 (2016). [PubMed: 26903601]
47. Ficz G et al. FGF signaling inhibition in ESCs drives rapid genome-wide demethylation to the epigenetic ground state of pluripotency. Cell stem cell 13, 351–359, doi:10.1016/j.stem.2013.06.004 (2013). [PubMed: 23850245]
48. Habibi E et al. Whole-genome bisulfite sequencing of two distinct interconvertible DNA methylomes of mouse embryonic stem cells. Cell stem cell 13, 360–369, doi:10.1016/j.stem.2013.06.002 (2013). [PubMed: 23850244]

49. Galonska C, Ziller MJ, Karnik R & Meissner A Ground State Conditions Induce Rapid Reorganization of Core Pluripotency Factor Binding before Global Epigenetic Reprogramming. Cell stem cell 17, 462–470, doi:10.1016/j.stem.2015.07.005 (2015). [PubMed: 26235340]
50. Bauer DE et al. Cytokine stimulation of aerobic glycolysis in hematopoietic cells exceeds proliferative demand. FASEB J 18, 1303–1305, doi:10.1096/fj.03-1001fje (2004). [PubMed: 15180958]
51. Frauwirth KA et al. The CD28 signaling pathway regulates glucose metabolism. Immunity 16, 769–777 (2002). [PubMed: 12121659]
52. Utsunomiya-Tate N, Endou H & Kanai Y Cloning and functional characterization of a system ASC-like Na+-dependent neutral amino acid transporter. J Biol Chem 271, 14883–14890 (1996). [PubMed: 8662767]
53. Kammen HO & Hurlbert RB Amination of uridine nucleotides to cytidine nucleotides by soluble mammalian enzymes; role of glutamine and guanosine nucleotides. Biochim Biophys Acta 30, 195–196 (1958). [PubMed: 13584420]
54. Marsboom G et al. Glutamine Metabolism Regulates the Pluripotency Transcription Factor OCT4. Cell Rep 16, 323–332, doi:10.1016/j.celrep.2016.05.089 (2016). [PubMed: 27346346]
55. Alexander PB, Wang J & McKnight SL Targeted killing of a mammalian cell based upon its specialized metabolic state. Proc Natl Acad Sci U S A 108, 15828–15833, doi:10.1073/pnas.1111312108 (2011). [PubMed: 21896756]
56. Finley LWS et al. Pluripotency transcription factors and Tet½ maintain Brd4-independent stem cell identity. Nat Cell Biol 20, 565–574, doi:10.1038/s41556-018-0086-3 (2018). [PubMed: 29662175]
57. Shi ZD et al. Genome Editing in hPSCs Reveals GATA6 Haploinsufficiency and a Genetic Interaction with GATA4 in Human Pancreatic Development. Cell stem cell 20, 675–688 e676, doi:10.1016/j.stem.2017.01.001 (2017). [PubMed: 28196600]
58. Millard P, Letisse F, Sokol S & Portais JC IsoCor: correcting MS data in isotope labeling experiments. Bioinformatics 28, 1294–1296, doi:10.1093/bioinformatics/bts127 (2012). [PubMed: 22419781]
59. Lengner CJ et al. Oct4 expression is not required for mouse somatic stem cell self-renewal. Cell Stem Cell 1, 403–415, doi:10.1016/j.stem.2007.07.020 (2007). [PubMed: 18159219]

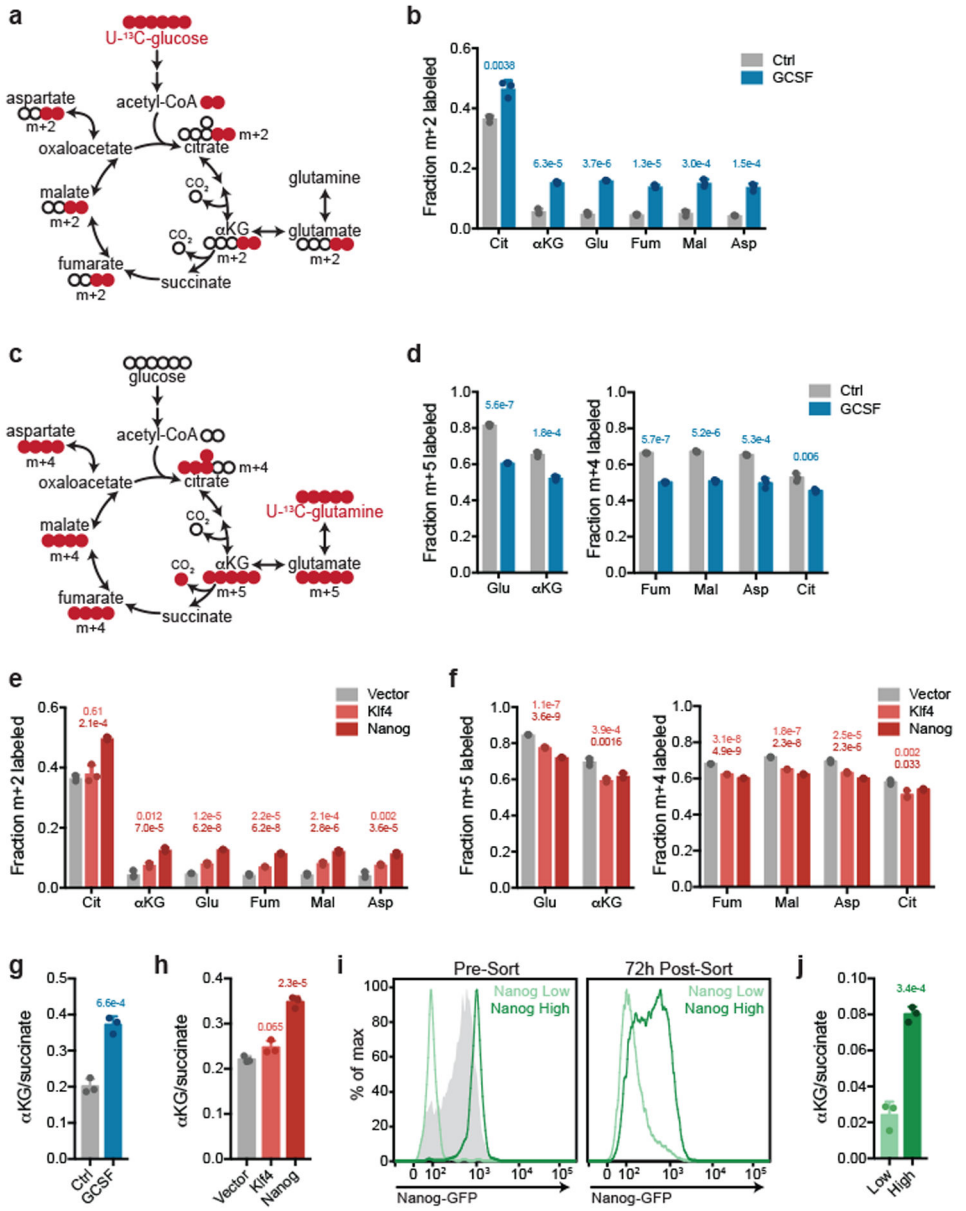

Figure 1. Glutamine anaplerosis is reduced in ESCs with enhanced self-renewal.

a,c, Schematics depicting how oxidative metabolism of uniformly-labeled glucose ([U-^{13}C]glucose (**a**)) and glutamine ([U-^{13}C]glutamine (**c**)) generates metabolites associated with the TCA cycle. Colored circles represent ^{13}C-labeled carbons. **b,e,** Fractional m+2 labeling of citrate (Cit), α-ketoglutarate (αKG), glutamate (Glu), fumarate (Fum), malate (Mal) and aspartate (Asp) in ESCs expressing GCSF-activated LIF receptor transgene cultured with or without GCSF (**b**) or ESCs expressing empty vector, Klf4 or Nanog (**e**) cultured in medium containing [U-^{13}C]glucose. **d,f,** Fractional m+5 labeling of Glu and αKG and m+4 labeling of Fum, Mal, Asp and Cit in ESCs expressing GCSF-activated LIF receptor transgene cultured with or without GCSF (**d**) or ESCs expressing empty vector, Klf4 or Nanog (**f**) cultured in medium containing [U-^{13}C]glutamine. **g,h,** Quantification of the αKG/succinate ratio in ESCs expressing GCSF-activated LIF receptor transgene

cultured with or without GCSF (**g**) or ESCs expressing empty vector, Klf4 or Nanog (**h**). **i,** Separation of Nanog Low and Nanog High populations by FACS. Left, shaded grey represents the parental Nanog-GFP population cultured in S/L medium; the top 10% and bottom 10% populations (outlined in green) were sorted and plated for subsequent experiments. Right, flow cytometry analysis of Nanog Low and Nanog High populations 72 h after initial sort. **j,** Quantification of the αKG/succinate ratio in Nanog Low and Nanog High populations shown in panel **i** (right). Experiment was repeated two independent times with similar results. *P* values were calculated by unpaired, two-sided Student's *t*-test (b,d,g,j) or one-way ANOVA with Sidak's multiple comparisons post-test (e,f,h) relative to control cells (b,d,e,f,g,h) or Nanog Low cells (j). Data are presented as the mean ± s.d. of n=3 biologically independent samples from a representative experiment (b,d,e,f,g,h,j).

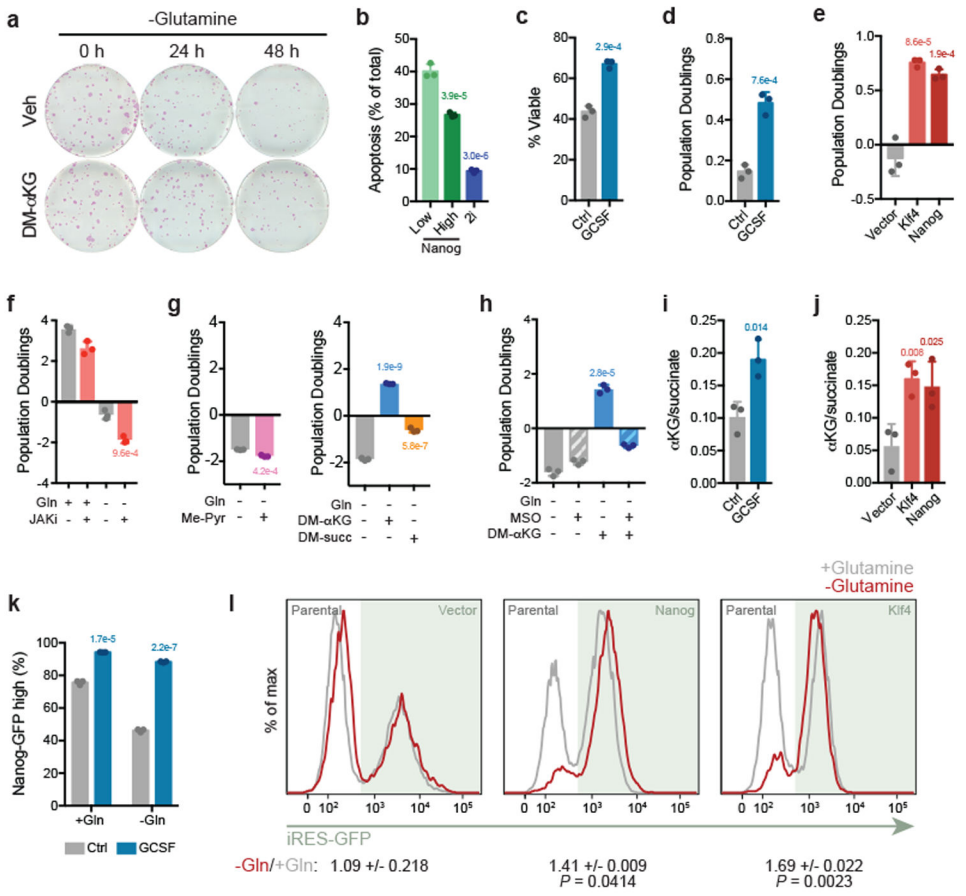

Figure 2. Enhanced self-renewal improves glutamine-independent survival.

a, Alkaline phosphatase staining of colony formation assays of ESCs subjected to glutamine withdrawal for the indicated times in the presence of DMSO (Veh) or dimethyl-α-ketoglutarate (DM-αKG). One representative well is shown. Experiment was repeated two independent times with similar results. **b,** Quantification of apoptosis in Nanog High and Nanog Low ESCs 72 h after sorting based on Nanog-GFP expression. Cells were deprived of glutamine for the final 24 h. **c,d** Viability (measured by DAPI exclusion) (**c**) or population doublings (**d**) of ESCs expressing GCSF-activated LIF receptor transgene cultured with or without GCSF and deprived of glutamine for 48 h. **e,** Population doublings of ESCs expressing empty vector, Klf4 or Nanog during 48 h of culture in glutamine-free medium. **f-h,** Population doublings of ESCs cultured for 48 h in glutamine-free medium unless otherwise noted. Where noted, the following compounds were included: JAKi, (ruxolitinib, 500 nM), DM-αKG (4 mM), dimethyl-succinate (DM-succ, 4 mM), methyl-pyruvate (Me-Pyr, 2 mM), or glutamine synthetase inhibitor methionine sulfoximine (MSO, 1 mM). **i,j,** Quantification of the αKG/succinate ratio in ESCs expressing GCSF-activated LIF receptor transgene cultured with or without GCSF following 8 h of glutamine deprivation (**i**) or ESCs expressing empty vector, Klf4 or Nanog following 4 h of glutamine deprivation (**j**). **k,** Fraction of Nanog-GFP ESCs expressing GCSF-activated LIF receptor transgene cultured with or without GCSF exhibiting high Nanog-GFP expression after culture in the presence or absence of glutamine for 48 h. **l,** Relative accumulation of GFP+ ESCs expressing empty

vector, Klf4, or Nanog compared to parental controls following culture in the presence of absence of 2 mM glutamine (+/−Gln) for 48 h. Ratio represents the fraction of GFP+ cells after culture −Gln relative to the fraction of GFP+ cells after culture +Gln. *P* values were calculated by unpaired, two-sided Student's *t*-test (c,d,f,g,h,i,k) or one-way ANOVA with Sidak's multiple comparisons post-test (b,e,j,l), relative to Nanog low cells (b), control ESCs (c,d,e,i,j,k,l), or cells cultured in glutamine-deficient medium alone (f,g,h). Data are presented as the mean ± s.d. of n=3 biologically independent samples from a representative experiment (b-l).

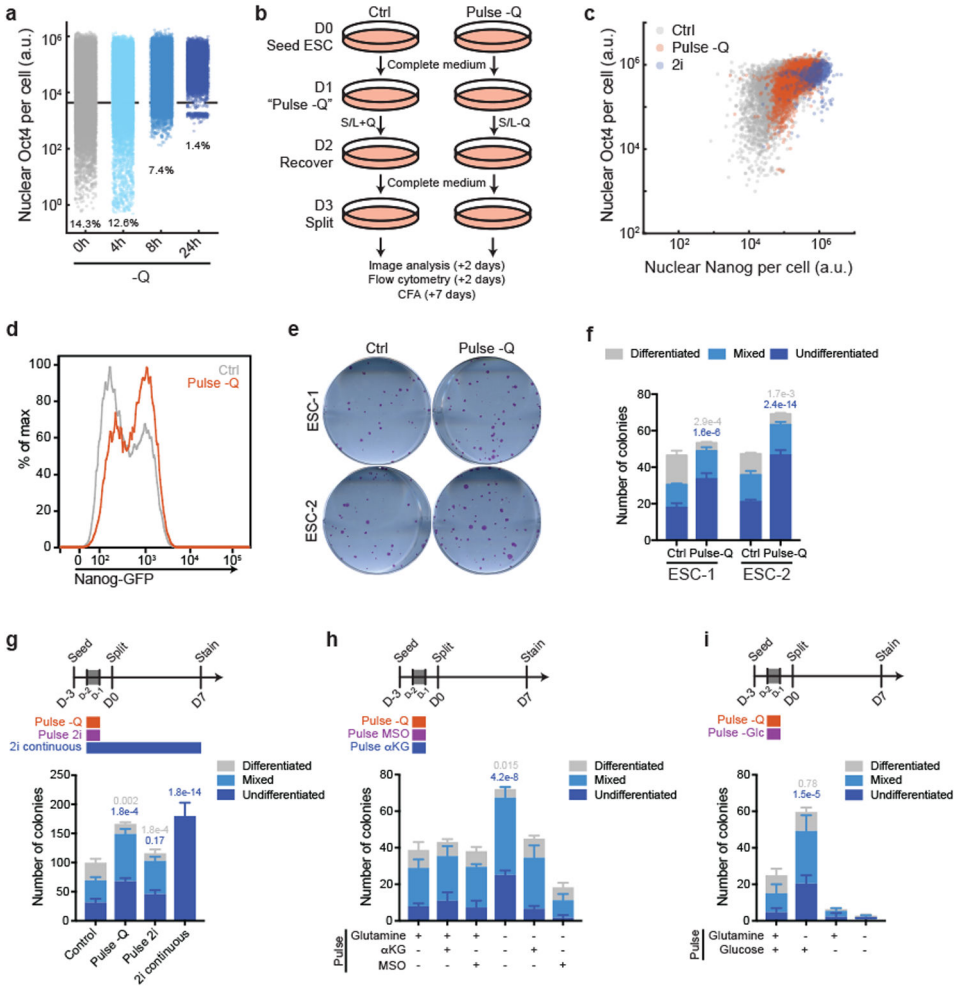

Figure 3. Transient glutamine withdrawal enhances ESC self-renewal.

a, Quantification of Oct4 immunofluorescence in ESCs cultured in the absence of glutamine (Q) for the indicated times. Dashed line denotes threshold for "Oct4 low" cells, defined as one standard deviation below the mean values of the control population. **b,** Experimental design for transient glutamine withdrawal ("Pulse −Q"). **c,** Quantification of Oct4 and Nanog immunofluorescence in control (Ctrl) or S/L+2i (2i)-cultured ESCs or ESCs previously subjected to 24 h of glutamine deprivation (Pulse −Q). **d,** Expression of Nanog-GFP in ESCs subjected to glutamine withdrawal for 24 h and then recovered with glutamine-replete medium for 24 h (Pulse −Q) or maintained in glutamine-replete medium (Ctrl). **e,** Alkaline phosphatase (AP) staining of colony formation assays in which two different ESC lines were maintained in glutamine-replete medium (Ctrl) or subjected to transient glutamine withdrawal for 24 h and then recovered in glutamine-replete medium for 24 h prior to plating (Pulse −Q). One representative well is shown. **f,** Quantification of colonies formed in (**e**). Colonies were scored manually as undifferentiated, mixed, or differentiated based on AP staining. **g-i,** Quantification of colony formation assays in which ESCs were maintained continuously in S/L medium containing glutamine (Control) or subjected to 24 h of glutamine withdrawal followed by recovery in control medium for 24 h prior to plating (Pulse −Q). Additional manipulations included exposing cells to 2i

continuously (2i continuous) or for 24 h (Pulse 2i) (**g**), the addition of 4 mM dimethyl-α-ketoglutarate (DM-αKG) or 1 mM methionine sulfoximine (MSO) during the "pulse" (**h**) and transient withdrawal of glutamine and/or glucose for 24 h followed by recovery in complete medium for 24 h prior to plating (**i**). *P* values were calculated by unpaired, two-sided Student's *t*-test (f) or one-way ANOVA with Sidak's multiple comparisons post-test (g,h,i), relative to control ESCs. Data are presented as the mean ± s.e.m. (f) or s.d. (g-i) of n=6 biologically independent samples from a representative experiment, or as >10,000 cells pooled from n=3 biologically independent samples from a representative experiment (a,c). Experiment was repeated two (a,c,e) or three (d) independent times with similar results.

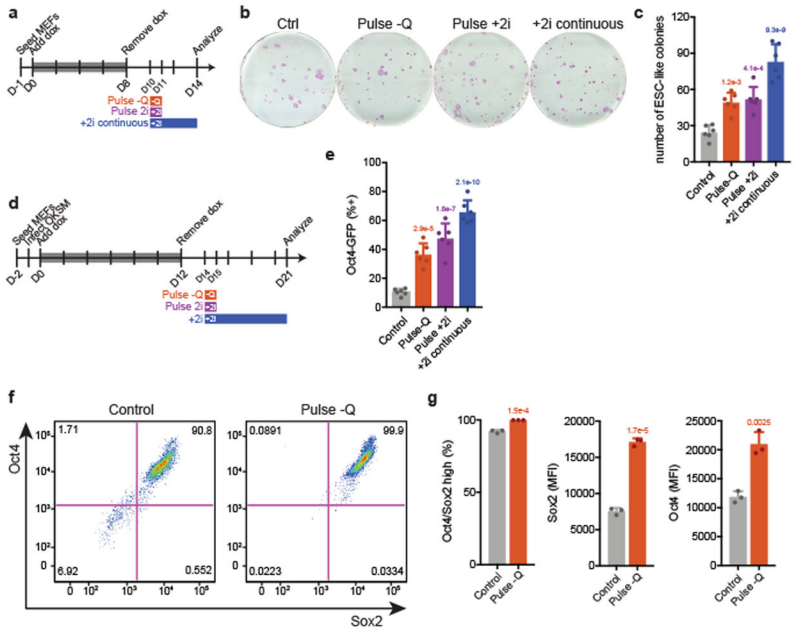

Figure 4. Transient glutamine withdrawal improves mouse somatic cell reprogramming to pluripotency and enhances human ESC self-renewal.

a, Experimental design for reprogramming of mouse embryonic fibroblasts (MEFs) expressing doxycycline (dox)-inducible Oct4, Sox2, Klf4 and c-Myc (OSKM). Cells were subjected to dox for 8 d. On day 10, cells were exposed to 2i for the duration of the experiment (+2i), 24 h of glutamine deprivation (Pulse −Q), 24 h of 2i (Pulse 2i), or maintained in glutamine-replete medium (Control). **b,** Alkaline phosphatase (AP) staining of a representative well of cells reprogrammed as described in (**a**). **c,** Quantification of the number of round, highly-AP stained colonies representing successfully reprogrammed colonies formed from OSKM-MEFs 14 d after initial dox addition. **d,** Experimental design for reprogramming of Oct4-GFP MEFs. Cells were infected with OKSM virus the day after seeding. The following day, cells began 12 d of dox exposure. On day 14, cells were exposed to 2i for the duration of the experiment (+2i), 24 h of glutamine deprivation (Pulse −Q), 24 h of 2i (Pulse 2i), or maintained in glutamine-replete medium (Control). **e,** Percentage of Oct4-GFP-expressing cells as an indicator of successful reprogramming at day 21 following initial dox induction. **f,** Expression of OCT4 and SOX2 in human ESCs subjected to glutamine withdrawal for 24 h and then recovered with glutamine-replete medium for 24 h (Pulse −Q) or maintained in glutamine-replete medium (Control). **g,** Quantification of OCT4 and SOX2 mean fluorescence intensity as well as percentage of OCT4/SOX2 high cells as depicted in (**f**). *P* values were calculated by unpaired, two-sided Student's *t*-test (g) or one-way ANOVA with Sidak's multiple comparisons post-test (c,e) relative to control ESCs maintained in glutamine-replete medium. Data are presented as the mean ± s.d. of n=6 (c,e) or n=3 (g) biologically independent samples from a representative experiment.